J. Fluid Mech. (1991), *vol.* 228, *pp.* 275–293
Printed in Great Britain

Shear flow of periodic arrays of particle clusters: a boundary-element method

By N. PHAN-THIEN,[1] T. TRAN-CONG[2] AND A. L. GRAHAM[3]

[1] Department of Mechanical Engineering, The University of Sydney, NSW 2006, Australia

[2] Department of Mechanical Engineering, University College of Southern Queensland, Toowoomba, Queensland 4350, Australia

[3] Division of Mechanical and Electronic Engineering, Los Alamos National Laboratory, Los Alamos, NM 87545, USA

(Received 23 May 1990 and in revised form 18 December 1990)

The boundary-element method is used to solve Stokes equations for periodic arrays of force-free and torque-free rigid particles. Simple cubic arrays of spheres, spheroids, cubes, and clusters of spheres are subjected to a bulk simple shearing flow. The effective volume-averaged stress tensor for the suspension and the detailed velocity and stress fields throughout the Newtonian suspending fluid are calculated. We find that even crude meshes give very good volume-averaged results, but fine meshes are required to track local minima and maxima in the stress field. For simple cubic arrays of spheres, the boundary-element results are in excellent agreement with the analytical viscosity predictions of Nunan & Keller (1984). Even at the highest concentration of solids studied, no significant normal stress differences were observed, in agreement with Nunan & Keller's results (1984). Up to moderate concentrations of particles, the volume-averaged properties of the suspension display only a weak dependence on the particle geometry. Suspensions of spheroids and cubes behave approximately as suspensions of spheres on the average despite large differences in the local micromechanics of stress and velocity fields. Simple cubic arrays of clusters of spheres tend to behave on a macroscopic level as a cubic array of spheres whose effective volume fraction is about 150 % of the total volume fraction of the spheres in the clusters.

1. Introduction

A central difficulty in understanding the mechanics of suspensions is the lack of knowledge concerning the hydrodynamic interaction of multiple particles suspended in a Newtonian fluid. The ultimate goal is the calculation of the effective transport properties of the bulk material considered as homogeneous on a macroscopic scale. Theoretical attempts to determine these effective transport properties have been successful in the limit of dilute systems (e.g. Batchelor 1970). In the systems of most practical interest, the least information is available.

In all existing theories of suspensions (e.g. Batchelor 1970, 1982; Jeffrey & Acrivos 1976; Herczyński & Pieńkowska 1980; Brenner, Nadim & Haber 1987), the inter-particle interaction is the essential ingredient. In a series of papers, Brenner (1963, 1964*a*–*c*) systematically analysed the problem of Stokes resistance of an arbitrary particle and showed that the hydrodynamic force and torque acting on such a particle can be expressed in terms of its translational and angular velocities, and the arbitrary imposed Stokes flow via the resistance functions (coefficients). Brenner &

O'Neill (1972) later generalized the results for a multiparticle system in a linear shear flow and defined the grand resistance matrix of the system.

Although the mathematical analyses mentioned above furnished a great deal of information concerning the dynamics of a multiparticle system, some detailed calculations and numerical values for the resistance functions (Brenner & O'Neill 1972) or the mobility functions defined by Batchelor (1976) were completed only recently. Kim & Mifflin (1985) considered two spheres of equal size in an arbitrary uniform rate-of-strain field. Two spheres of unequal sizes in a uniform field plus a superposed rigid-body motion were studied by Jeffrey & Onishi (1984). Kim (1987) reported an analytic solution for the Stokes flow problem past three equal spheres fixed at the vertices of an equilateral triangle.

Ganatos, Pfeffer & Weinbaum (1978) extended the collocation technique developed by Gluckman, Pfeffer & Weinbaum (1971) and Leichtberg *et al.* (1976*a–b*) and solved for the motion of a large number of interacting spheres lying in a plane. Bloomfield, Dalton & Holde (1967) proposed a shell model whereby a particle is modelled by an assembly of identical spherical elements, distributed on a surface shell derived from the shape of the particle. McCammon & Deutch (1976) computed the Stokes drag on a particle by solving a set of linear algebraic equations of the Kirkwood–Riseman type (Kirkwood & Riseman 1948). Subsequent development along this line, by Swanson, Teller & Haën (1978), Roger & Hussey (1982), gave rise to the so-called beads-on-a-shell method. The problem involving more than two spheres in an arbitrary configuration was treated by Kynch (1959) and Mazur & van Saarloos (1982) using a power series expansion in R^{-1}, where R is a typical particle spacing. Beenakker (1984) used these results to study the effective viscosity of a concentrated suspension of spheres, taking into account the multiparticle hydrodynamic interaction.

Recently Durlofsky, Brady & Bossis (1987) and Brady & Bossis (1988) developed a very efficient technique termed the Stokesian Dynamics method for modelling a cluster of spherical particles in an arbitrary Stokes flow. The method involves adding the inverse of the far-field mobility matrix of two sphere interactions to the resistance matrix of two sphere lubrication resistance functions and solving the resulting equations. Although the method is approximate, the results obtained so far have proved to be accurate and useful in elucidating several mechanisms at work in flows of suspensions. The method is, however, designed for spheres since the far-field and near-field resistance functions are available for spheres only.

An infinite number of spheres arranged periodically can be treated analytically (Zick & Homsy 1982; Nunan & Keller 1984; Adler, Zuzovsky & Brenner 1985; Brady *et al.* 1988). Nunan & Keller (1984) showed that the deviatoric average stress in a periodic suspension is linear in the average strain rate. On average, the fluid is anisotropic with a fourth-order tensorial effective viscosity, which is related to the lattice geometry and the volume fraction via two scalar functions, α and β. Asymptotic formulae as well as numerical values for α and β were given for a number of lattices. The numerical method is based on solving a set of integral equations that were derived by using a periodic singularity solution of Hasimoto (1959). The method is therefore a boundary-integral-equation method (see, for examples, Banerjee & Butterfield 1981; Brebbia, Telles & Wrobel 1984), except that the kernel used in these integral equations is quite complicated and involves a lattice sum. Nunan & Keller (1984) adopted a Galerkin method used by Zick & Homsy (1982) for solving the resulting set of integral equations, and they were able to obtain numerical results up to 90% of maximum volume fraction. Their numerical results agree well with the asymptotic results at low volume fractions (Adler *et al.* 1985) and their own asymptotic results at high volume fractions. Brady *et al.* (1988) adapted the Stokesian Dynamics method to simulate the flow of an infinite suspension of hydrodynamically interacting spheres. The method yields excellent results when compared to the exact solutions of Saffman (1973), Zick & Homsy (1982), and Nunan & Keller (1984) for the sedimentation, permeability, and viscosity problems of periodic suspensions. In particular for the viscosity problem, their method reproduces the exact behaviour at high volume fractions. The Stokesian Dynamics method is undoubtedly the best available method for simulating an infinite suspension of spheres.

The use of the boundary-integral-equation method, or boundary-element method (BEM) in solving Stokes problems was first reported by Gluckman, Weinbaum & Pfeffer (1972) for an arbitrary convex body of revolution, and by Youngren & Acrivos (1975) for an arbitrary rigid particle. The distinctive advantage of the method over traditional methods, such as finite difference and finite element, is a reduction of dimensionality afforded by converting the original set of three-dimensional partial differential equations into a set of integral equations defined on the boundary of the solution domain. The resulting system matrix, although fully populated, is usually small in size compared to corresponding systems generated by the finite-difference or finite-element methods. The BEM has been successfully employed in solving a number of three-dimensional Stokes flow problems. These include the swimming of spermatozoa (Phan-Thien, Tran-Cong & Ramia 1987), the sedimentation of spheroidal particles near a planar interface (Tran-Cong & Phan-Thien 1989), the flow between two parallel plates past a two-dimensional periodic array of force-free and torque-free spheroids (Tran-Cong, Phan-Thien & Graham 1990), the flow of a cluster of spheres in a cylinder (Ingber, Mondy & Graham 1989), the extrusion problem for Newtonian (Bush & Phan-Thien 1984; Tran-Cong & Phan-Thien 1988*a*) and viscoelastic fluids (Tran-Cong & Phan-Thien 1988*b*), and the three-dimensional die-design problem (Tran-Cong & Phan-Thien 1988*c*).

In this paper we extend the BEM to simple shearing flow of a three-dimensional periodic array of force- and torque-free particles. The BEM cannot compete with the Stokesian Dynamics method (Durlofsky *et al.* 1987; Brady & Bossis 1988; Brady *et al.* 1988) in terms of efficiency, but it is general and can be applied to a system of non-spherical particles of different sizes and shapes. Furthermore, the detailed kinematics and stress field can be readily obtained by a post-processing of the boundary solution. The method is benchmarked against the numerical and asymptotic results of Nunan & Keller (1984) and new results for periodic arrays of spheroids, cubes, and clusters of spheres are reported. It is found that the BEM results agree well with the numerical results of Nunan & Keller (1984). The instantaneous effective viscosity is only weakly dependent on the particle shape at volume fraction not near to the maximum packing. We find that the instantaneous viscosity of some periodic arrays of clusters of spheres is about the same as the instantaneous viscosity of a cubic array of spheres provided that the volume fraction Φ of the clusters is replaced by an effective volume fraction $\Phi_{eff} \approx 1.5\Phi$. This is essentially Roscoe's conclusion (1952), although the empirical relation reported was $\Phi_{eff} \approx \Phi/\Phi_{max}$, where Φ_{max} is the maximum volume fraction for the type of packing assumed in the cluster; $1/\Phi_{max}$ ranges from 1.35 for a face-centred cubic packing to 1.47 for a body-centred cubic packing, and to 1.91 for a simple cubic packing.

2. Basic equations

We consider a set of rigid, neutrally buoyant particles arranged periodically in a three-dimensional lattice. The particles are suspended in a Newtonian fluid of viscosity η and undergoing a bulk simple shearing flow in the xz-plane. The flow is assumed to be isothermal and without body forces so that in the region E containing the fluid, the pressure P, the velocity $\boldsymbol{u}$, and the stress tensor $\boldsymbol{\sigma}$ satisfy the Stokes equations.

Owing to the periodicity of the solution, it is sufficient to consider a unit cell determined by the basis vectors $\{\boldsymbol{a}_i\}$, $i = 1, 2, 3$. Periodicity conditions are imposed on any multiple of a linear combination of the basis vectors. More precisely, if $\boldsymbol{r}^\alpha = \alpha_1 \boldsymbol{a}_1 + \alpha_2 \boldsymbol{a}_2 + \alpha_3 \boldsymbol{a}_3$, where α_i can be any integer, then the following boundary condition is imposed:

$$\boldsymbol{u}(\boldsymbol{x}+\boldsymbol{r}^\alpha) = \boldsymbol{u}(\boldsymbol{x}) + \dot{\boldsymbol{\gamma}}\cdot\boldsymbol{r}^\alpha. \tag{1}$$

In (1), $\dot{\boldsymbol{\gamma}}$ is the bulk velocity gradient tensor applied to the flow (Batchelor 1970). In this paper we are only concerned with a bulk simple shearing flow and the only non-zero component of $\dot{\boldsymbol{\gamma}}$ is $\dot{\gamma}_{13} = \dot{\gamma}$, i.e. the bulk shearing flow takes place in the xz-plane. The bulk shear rate $\dot{\gamma}$ is normalized to unity.

In addition, the particles in a unit cell are free to move, subjected to the force- and torque-free conditions. We are concerned with the mobility problem, and finding the translational and the angular velocities of particle i, $\boldsymbol{U}_i$ and $\boldsymbol{\Omega}_i$, respectively, is part of the solution procedure.

The problem is now well-posed, and analytic solution is possible for some simple lattices (Nunan & Keller 1984). Our numerical scheme deals with the unit cell directly and therefore some relevant boundary conditions for the traction vector are needed on the surface of the unit cell (these are not required in the analytic solution). The periodicity of the fluctuating velocity and the pressure fields (there is no intrinsic pressure gradient in this problem) implies that the fluctuating stress tensor is also periodic:

$$\boldsymbol{\sigma}(\boldsymbol{x}+\boldsymbol{r}^\alpha) = \boldsymbol{\sigma}(\boldsymbol{x}) + \eta(\dot{\boldsymbol{\gamma}}+\dot{\boldsymbol{\gamma}}\dagger). \tag{2}$$

The constraint on the traction vector on the boundary of the unit cell, $\boldsymbol{t} = \boldsymbol{n}\cdot\boldsymbol{\sigma}$, where $\boldsymbol{n}$ is the outward unit vector on the bounding surface of the unit cell, can be easily derived from the periodicity of the fluctuating stress tensor and the geometry of the unit cell.

Suppose that the fluid motion has been found. Then, as shown by Batchelor (1970), the volume-averaged stress tensor is given by

$$\langle\boldsymbol{\sigma}\rangle = -\langle P\rangle \boldsymbol{I} + \eta(\dot{\boldsymbol{\gamma}}+\dot{\boldsymbol{\gamma}}\dagger) + \boldsymbol{\tau}, \tag{3}$$

where the angular brackets denote a volume average and $\boldsymbol{\tau}$ is the effective stress contributed by the particles at the instant considered. It is given by

$$\boldsymbol{\tau} = \frac{1}{V}\int_S (\boldsymbol{x}\boldsymbol{\sigma}\cdot\boldsymbol{n} - \tfrac{1}{3}\boldsymbol{x}\cdot\boldsymbol{\sigma}\cdot\boldsymbol{n}\boldsymbol{I})\,\mathrm{d}S. \tag{4}$$

Here V is the volume of the periodic cell, taken as a representative volume, S is the bounding surface of V, which includes the bounding surfaces of all particles contained in V, and $\boldsymbol{I}$ is the unit tensor.

The determination of the effective properties of the suspension entails solving the boundary-value problem for the microstructure and calculating relevant ensemble averages over all possible configurations of the particles. Here, only one possible configuration of the particles is considered and therefore we refer to the volume-averaged properties as instantaneous effective, or simply effective, properties. Thus the instantaneous reduced viscosity of the periodic suspension can be defined as

$$\chi = \frac{\langle \sigma \rangle}{\eta \dot{\gamma}} = 1 + \frac{\tau_{xz}}{\eta \dot{\gamma}}. \tag{5}$$

The governing equations are recast in integral form using the standard Stokeslet singular solution (see, for examples Banerjee & Butterfield 1981, or Brebbia *et al.* 1984). It is possible to use a special periodic singular solution derived by Hasimoto (1959) and therefore satisfy the periodic boundary conditions exactly. However, the periodic kernel depends on a lattice sum and is less flexible for our purposes.

With velocity boundary conditions the resulting integral equations are of the first kind in terms of the boundary tractions. This can lead to an ill-conditioned algebraic system upon discretization. The cause of the ill-condition problem has been clearly expounded by Karrila & Kim (1990) for spheres. They find that the high spatial frequency inputs in the traction vector of the form $\nabla_s P_n^m(\cos\theta)\, e^{im\phi}$, where ∇_s is the surface gradient and P_n^m is the associate Legendre polynomial, are mapped to small outputs which vanish as $O(n^{-1})$. The inverse problem of finding the inputs (traction) knowing the outputs is therefore ill-conditioned. Karrila & Kim (1990) prefer an indirect integral formulation which they termed the Completed Double Layer Boundary Integral Equation Method, which always results in a set of integral equations of the second kind.

Despite these negative remarks on the ill-conditioned problem of the standard BEM for the case where boundary velocities are prescribed, we find that a good quality solution can be obtained for a system of particles in Stokes flow provided that the number of boundary elements is not large (less than about 10^3). The total number of elements is usually set by the physical amount of memory in the computer rather than the ill-posedness of the problem; one usually obtains a good quality solution before the ill-conditioned problem sets in (Tran-Cong *et al.* 1990).

A numerical implementation of the set of integral equations was reported in Tran-Cong *et al.* (1990). In this periodic-flow problem neither the boundary traction nor the velocity vectors are known on the boundary ∂E. On the boundary of the unit cell, however, they are related by the imposed periodic boundary conditions. These boundary conditions provide $6N$ equations, where N is the number of elements on the surface of the unit cell, which are also imposed. The force- and torque-free conditions can now be used to solve for the translational and angular velocities of each particle in the unit cell. The global traction vector, the velocity, the stress fields and the effective stress tensor contributed by the particles can then be evaluated.

3. Results and discussion

3.1. *Single particle*

The program is first tested with a single sphere (of radius $a = 1$) sedimenting along the z-direction in an unbounded body of fluid. Integral properties (force and torque on the particle for the resistant problem, and sedimentation velocity for the mobility problem) are predicted accurately with a crude mesh. We subjected the program to a stricter test of point-wise values of the velocity and the stress fields. With an 80-element sphere, the point-wise error in the kinematics is less than 3 %, and the point-wise error in the stress field is less than 11%, up to a distance of 10 radii from the sphere. The point-wise error in the kinematics is reduced to within 0.8% when a 320-element sphere is used. The maximum point-wise error in the stress field, however, is still of the order 8%. The maximum error in σ_{rr} occurs at the poles, at a distance of about 1.2 a from the sphere centre, where σ_{rr} attains its local maximum. The slow decay of the error in the stress field is due to the fact that the kernels involved in the integral equations for the stresses are more singular than the Stokeslet (they are the gradients of the Stokeslet). Integral properties are predicted accurately, to within 3% for an 80-element sphere.

If the problem can be assumed axi-symmetric, and the corresponding axi-symmetric kernels are used in the calculation, then the rate of convergence to the Stokes solution is more than quadratic in the number of elements, as table 1 shows. The rate of convergence to the Stokes solution is somewhat less than linear in the number of elements in the full three-dimensional problem. We also present some results for the axi-symmetric flow perpendicular to an oblate spheroid of aspect ratio 1000, and parallel to a prolate spheroid of aspect ratio 1000. Compared to the exact solution (Happel & Brenner 1973), the rate of convergence is about quadratic for these cases.

The pressure field on the sphere surface is also predicted accurately. With an 80-element sphere the error on the maximum pressure on the sphere surface (which occurs at the poles) is about 6%. This reduces to less than 1% with a 320-element sphere. The program has also been tested with more than one particle in an unbounded body of fluid, and near a planar interface (Tran-Cong & Phan-Thien 1989). The numerical results compare well with all available analytical solutions. It should be noted that in the sedimentation problem, our integral equation formulation leads to a set of integral equations of the first kind. An ill-conditioned problem will arise if the total number of elements is too large (of the order 10^3) when the particles are touching. The maximum number of elements used in this paper is 780, in the case of a periodic array of a cluster of six spheres. Within this constraint, however, we are still able to cover a range of volume fraction of interest and produce good quality numerical solutions.

3.2. *Cubic array of spheres*

We now consider the bulk shearing flow past a cubic array of force- and torque-free spheres. The problem has been considered by Nunan & Keller (1984) who showed that the effective stress contributed by the particle is linear in the bulk strain rate. The instantaneous effective viscosity is a fourth-order tensor which depends on two scalar functions of the volume fraction and the lattice geometry. The effective volume-averaged constitutive equation takes the form

$$\tau_{ij} = \eta(1+\beta)(\dot{\gamma}_{ij}+\dot{\gamma}_{ji})+\eta(\alpha-\beta)\,\delta_{ijkl}(\dot{\gamma}_{kl}+\dot{\gamma}_{lk}),$$

where δ_{ijkl} is unity if all the subscripts are equal and zero otherwise, and α and β are functions of the concentration and the lattice geometry (Nunan & Keller 1984). The bulk suspension is therefore anisotropic. In the bulk shearing flow considered here, the instantaneous reduced viscosity is given by

$$\chi \equiv \frac{\sigma_{xz}}{\eta\dot{\gamma}} = 1+\beta, \tag{6}$$

and the normal stress differences ($N_1 \equiv (\sigma_{xx}-\sigma_{\zeta\zeta})$ and $N_2 \equiv (\sigma_{zz}-\sigma_{yy})$) are zero. In a bulk elongational flow, the elongational viscosity is $\eta(1+\alpha)$.

	Sphere		Oblate		Prolate	
N	D/D_0	Error	D/D_0	Error	D/D_0	Error
20	0.99747	0.253				
30	0.99887	0.113	0.51080	0.489	0.57570	0.424
40	0.99935	0.0650				
50	0.99957	0.0427				
60	0.99970	0.0305				
72	0.99980	0.0197				
90	0.99987	0.0126	0.66337	0.337	0.84888	0.151
120	0.99993	0.00712				
180	0.99997	0.00317	0.90335	0.0966	1.01106	0.0111
240	0.99998	0.00179				
300	0.99999	0.00114	0.98780	0.0122	1.01361	0.0136
360	0.99999	0.000786	0.99581	0.00419	1.00855	0.00855
500	1.00000	4.10×10^{-6}	0.99966	0.000337	1.00292	0.00292
720	1.00000	1.94×10^{-6}	1.00002	1.94×10^{-5}	1.00086	0.000857

TABLE 1. Stokes flow past a sphere, perpendicular to an oblate spheroid, and parallel to a prolate spheroid (both of aspect ratio 1000) in an unbounded body of fluid. D/D_0 is the normalized Stokes drag (to five significant digits), which should be exactly one, and N is the total number of constant elements.

Numerical values for β and α are given for a number of simple lattices in Nunan & Keller (1984). Asymptotic results at low and high volume concentrations are also given. In particular, at high volume fraction and for a simple cubic lattice, they showed that

$$\beta = \tfrac{1}{4}\pi \ln \epsilon^{-1} + 0.63 + O(\epsilon), \tag{7}$$

where $\epsilon = 1-(\Phi/\Phi_{max})^{\frac{1}{3}}$; Φ and Φ_{max} are the volume fraction and the maximum volume fraction, respectively. For a simple cubic array, $\Phi_{max} = \frac{1}{6}\pi$. We find that the asymptotic result (7) does not agree with Nunan & Keller's numerical result even though their figure 2 shows that the two overlap in the region where the volume fraction is of the order 0.3. For example, at a volume fraction of 0.28, (7) gives $\beta =$ 1.94, whereas Nunan & Keller's numerical result is 0.744. Without checking their asymptotic results in detail, we think that the term $+0.63$ in (7) should be -0.63 which in the above example would produce $\beta = 0.68$, which is indistinguishable from their results shown on their figure 2. This corrected asymptotic relation will be used in the comparison with our numerical results.

The number of elements on the bounding surface of the unit cell is varied from 40 to 300, and the number of elements on the sphere is varied between 20 and 320 to gauge the convergence of the numerical solution. It is found that integral properties (i.e. instantaneous effective viscosity) are rather insensitive to the number of elements used. For volume fractions less than 0.45, a 20-element sphere in a 300-element unit cell produces results in excellent agreement with Nunan & Keller's numerical and asymptotic solutions. This is shown in figure 1. With an 80-element sphere in a 300-element unit cell, the instantaneous effective viscosity is within 0.9% of Nunan & Keller's asymptotic result at a volume fraction of 0.45 (Nunan & Keller only reported numerical results up to a volume fraction of 0.28). At high volume fractions (>0.45), more elements are needed on the sphere for convergence. It is found that a 320-element sphere in a 300-element unit cell can produce results in excellent agreement with the asymptotic formula, up to a volume fraction of 0.50,

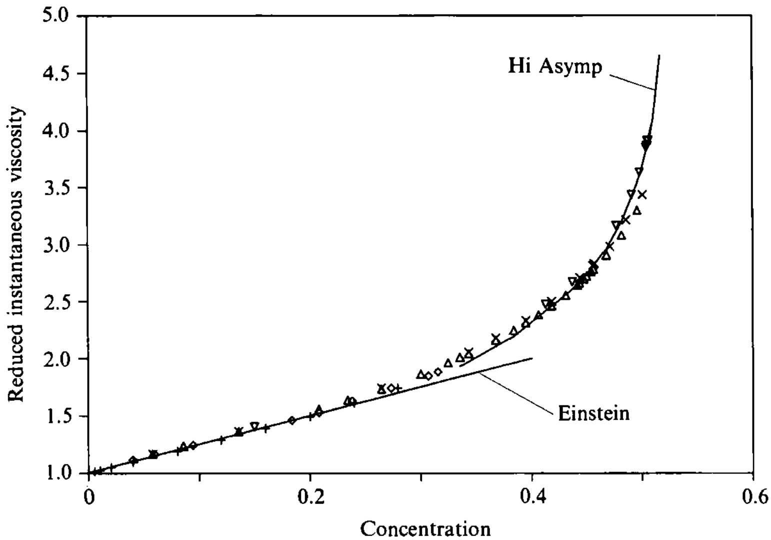

FIGURE 1. The reduced instantaneous viscosity (χ) as a function of the volume fraction. Excellent agreement with the numerical and asymptotic results of Nunan & Keller (1984) is noted. At a volume fraction of 0.505, which is about 96% of the maximum volume fraction, the reduced instantaneous viscosity predicted with a 320-element sphere in a 300-element unit cell is 3.87, which is 0.9% higher than the (corrected) asymptotic result of Nunan & Keller (1984). $\diamond$, 20-element sphere; $\triangle$, 80-element sphere; $\times$, 160-element sphere; ∇, 320-element sphere; $+$, Nunan & Keller (1984) results.

which is 95% of the close-packing concentration. At this volume fraction, the sphere is only 0.02 radius away from the wall of the unit cell. The ill-conditioned problem does not seem to affect the quality of the integral properties.

At low volume fractions, there are several asymptotic results, up to $O(\Phi^{\frac{10}{3}})$ due to Zuzovsky (1976) and Zuzovsky, Adler & Brenner (1983). Our results agree well with those results up to a volume fraction of about 0.25. Einstein's result,

$$\chi = 1 + 2.5\Phi, \tag{8}$$

works surprisingly well for volume fractions less than 0.25 (figure 1); the maximum error (compared to the numerical solution and Nunan & Keller's results) is less than 1% at $\Phi = 0.25$.

Nunan & Keller (1984) showed that the angular velocity of the sphere is exactly half of the curl of the average velocity, independence of the volume fraction (half, in this case, because the shear rate is normalized to unit). This is the same angular velocity that would be exhibited by a single sphere in an unbounded body of fluid subjected to the same volume-averaged strain rate. That is, each sphere in the cubic array spins as if other spheres were not there. For an 80-element sphere in a 300-element unit cell, we find that the sphere spins at an angular velocity in the range 0.498–0.502, which is about 0.4% from the exact value, for the whole range of volume fractions considered.

The detailed kinematics and stress field can be easily post-processed in the BEM. The surface contours of the velocity field show that the flow takes place mainly in the xz-plane, with the magnitude of the y-component of the velocity of the order 10^{-2} or less everywhere. The surface contours of the pressure and the stresses show that high-stress regions are found on the surface of the unit cell, near the poles. We find from

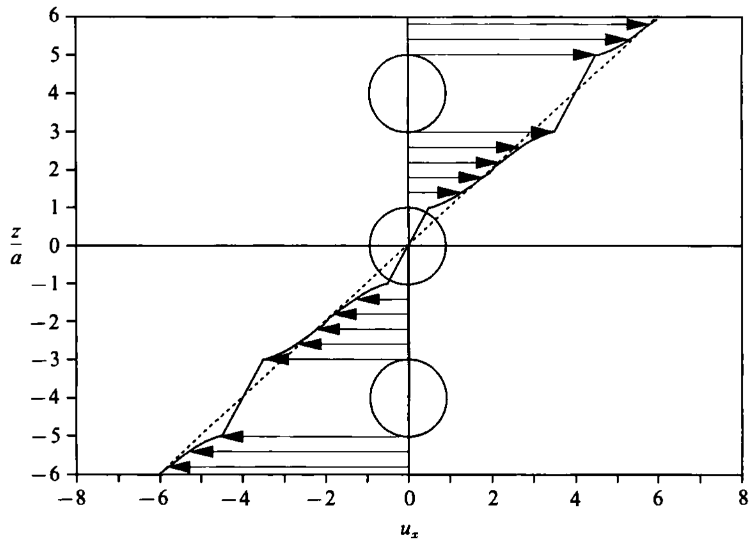

FIGURE 2. The velocity profile (u_x) along the z-axis for three consecutive periodic cells at $\Phi = 0.058$. The dashed line is the unperturbed shear flow.

the contours of velocities in the flow domain that the flow is mainly in the xz-plane, with no recirculation region in the unit cell.

The velocity component u_x along the z-axis along three neighbouring periodic cells are reconstructed in figure 2. The undisturbed shear flow ($u_x = z$) is also plotted in the same figure as a dashed line for comparison. The deviation from the undisturbed shear flow occurs periodically, with the maximum deviation occurring at the spheres' surfaces. This maximum deviation is exactly 0.5 $a\dot{\gamma}$, since the spheres rotate with the same angular velocity of 0.5 $\dot{\gamma}$. The odd symmetry of u_x with respect to $\zeta = z/a$ is evident in the figure and is due to the symmetry in the Stokes equations and the boundary conditions.

At all volume fractions considered, the effective normal stress differences are found to be negligible, being of the order 10^{-2} of the effective shear stress. This agrees with Nunan & Keller's solution.

Tran-Cong *et al.* (1990) considered a shear flow of a two-dimensional periodic array of three-dimensional spheres (in the x- and y-directions) but with only a finite number of layers between the containing walls. It is of interest to find out the number of layers of spheres that one needs to approximate a cubic array of spheres in all three directions. This can be determined by first calculating the effective viscosity of a mono-layer of spheres undergoing a simple shearing flow between two parallel plates. The number of layers can then be increased, keeping the volume fraction fixed until the effective viscosity converges to a definite value. All the spheres were included in the calculation of the particle contribution to the effective viscosity. We find that the instantaneous effective viscosity is about 2% greater than the three-dimensional cubic array's result for five layers of spheres. The five spheres in the unit cell do not contribute equally to the effective viscosity. The centre sphere behaves as if it was part of a lattice of infinite extent; the spheres in the intermediate and the bordering layers contribute relatively more (up to 1% more) to the effective viscosity than the centre sphere. Thus, in an integral sense, a sphere in a cubic array can only see about two nearest neighbours. This is a direct numerical confirmation of the shielding principle to which Stokesian Dynamics simulation (Brady & Bossis 1988; Brady *et al.* 1988; Durlofsky *et al.* 1987) owes much of its success.

We have established in this section that the standard BEM can be applied to a periodic Stokes flow problem, giving excellent results in the case of the flow past a cubic array of force- and torque-free spheres. The computational cost is not high, considering that we use a standard Gauss elimination to solve the resulting system of equation. A problem with 700 elements takes about 10 min to solve on a Cray-XMP, or about 200 min on a MIPS-120 workstation.

3.3. *Cubic array of spheroids*

We now consider a cubic array of prolate and oblate spheroids. The aspect ratio (ratio of major to minor radius) is chosen to be two. Three different orientations of the spheroids are considered:

aligned in the x-direction: the major (minor) axis of the prolate (oblate) spheroid is pointing in the x-direction;
aligned in the y-direction: the major (minor) axis of the prolate (oblate) spheroid is pointing in the y-direction;
aligned in the z-direction: the major (minor) axis of the prolate (oblate) spheroid is pointing in the z-direction.

In all cases the bulk shear flow takes place in the xz-plane with an average shear rate of 1, and the unit cell is the cube $E = \{x, y, z\colon -h < x < h,\ -h < y < h,\ -h < z < h\}$.

A mesh refinement study indicates that one needs only 80 elements on the spheroid in a 300-element unit cell to obtain good average results up to a volume fraction of 90% of the close packing concentration (for prolate spheroids of aspect ratio 2 this is $\frac{1}{24}\pi$, and for oblate spheroids of the same aspect ratio, it is $\frac{1}{12}\pi$).

The general form of the particle-contributed for a dilute suspension of spheroids was given by Batchelor (1970). Thus,

$$\tau = \frac{4\eta\Phi}{I_1}\left\{\frac{J_1}{J_2}(\boldsymbol{pp}-\tfrac{1}{3}\mathbf{1})\,\boldsymbol{D}:\boldsymbol{pp}+\boldsymbol{D}-\boldsymbol{pp}\cdot\boldsymbol{D}-\boldsymbol{D}\cdot\boldsymbol{pp}\right.$$
$$\left.+(\boldsymbol{pp}+\tfrac{1}{3}\mathbf{1})\boldsymbol{D}:\boldsymbol{pp}+\frac{I_1}{I_2}(\boldsymbol{pp}\cdot\boldsymbol{D}+\boldsymbol{D}\cdot\boldsymbol{pp}-2\boldsymbol{D}:\boldsymbol{pppp})\right\}, \quad (9)$$

where $\boldsymbol{p}$ is a unit vector parallel to the axis of revolution of the spheroid, $\boldsymbol{D}$ is the strain rate tensor, and I_i, J_i are integrals that depend only on the shape of the spheroid; they are defined in Batchelor (1970). At an aspect ratio of 2, these integrals can be evaluated, leading to an effective reduced viscosity of $1+2.504\Phi$, for prolate spheroids aligned in the x- and z-direction, $1+2.174\Phi$, for prolate spheroids aligned in the y-direction, $1+2.063\Phi$, for oblate spheroids aligned in the x- and z-direction, and $1+3.267\Phi$, for oblate spheroids aligned in the y-direction. Note that the effective viscosity of suspensions of spheroids aligned in the x- and in the z-direction is the same. This follows from the fact that the rate of strain tensor is the same in both cases, apart from a trivial rigid rotation, after a suitable change of frame.

The main results for prolate spheroids are summarized in figure 3, where the instantaneous effective viscosity and the particle angular velocity are plotted against the reduced volume fraction (Φ/Φ_{max}). We find that the effective viscosity of suspensions of spheroids aligned in the x- and z-direction is the same to three significant digits. This follows from the observation noted above and the symmetry of the cubic array. The asymptotic limits at low volume fractions for the case of

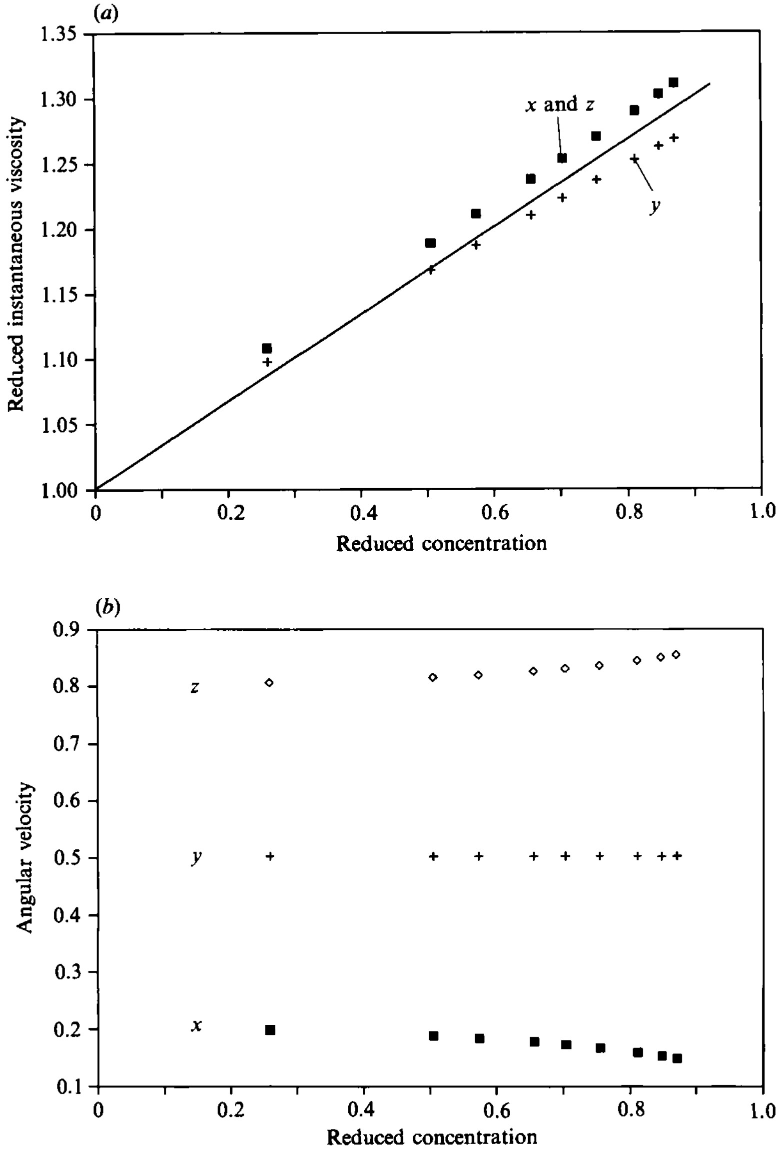

FIGURE 3. The instantaneous reduced viscosity (a) and the angular velocity (b) of a cubic array of prolate spheroids of aspect ratio of 2. Eighty elements were used to model the spheroid and 300 elements were used to model the unit cell. Note that the instantaneous viscosities of cubic arrays of spheroids aligned in the x-direction and in the z-direction are about the same. Their angular velocities are different though, and they tend to the correct limits predicted by Jeffery's solution (1922). The maximum volume fraction in this case is $\frac{1}{24}\pi$. ■, align in x-direction; +, align in y-direction; ◇, align in z-direction.

spheroids aligned in x- and z-direction are also included in figure 3(a) for comparison. The numerical results are about 2% higher than the asymptotic results; this systematic error is due to the discretization errors.

From figure 3(b), the spheroids aligned in the z-direction rotate with the fastest angular velocity ($\approx 0.8\dot{\gamma}$), those aligned in the x-direction rotate with the slowest angular velocity ($\approx 0.2\dot{\gamma}$), and those aligned in the y-direction rotate just like a

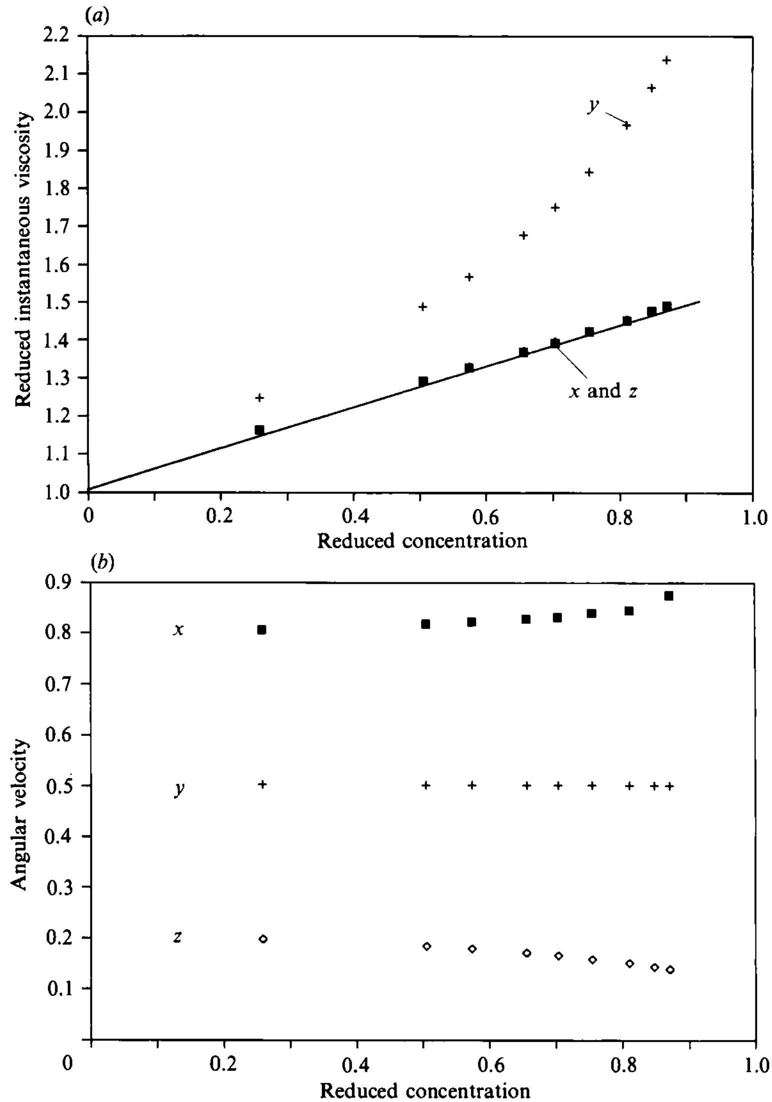

FIGURE 4. Same as in figure 3 (*a*, *b*), but for a cubic array of oblate spheroids of aspect ratio 2. The maximum volume fraction in this case is $\frac{1}{12}\pi$. ■, align in *z*-direction; +, align in *y*-direction; ◇, align in *x*-direction.

sphere, with an angular velocity of about $0.5\dot{\gamma}$. The quoted angular velocities are also the asymptotic limits at low volume fractions (Jeffery 1922). The angular velocities of the spheroids are only weakly-dependent on the volume fraction.

The results for oblate spheroids are summarized in figure 4. Here, one finds that the numerical results agree well with asymptotic results for the whole range of volume fraction considered.

3.4. *Cubic array of cubes*

We now consider a cubic array of cubes. A mesh refinement study shows that we need only a 48-element cube to obtain good averaged results up to a volume fraction of 90%. The instantaneous effective viscosity of a cubic array of cubes perfectly aligned

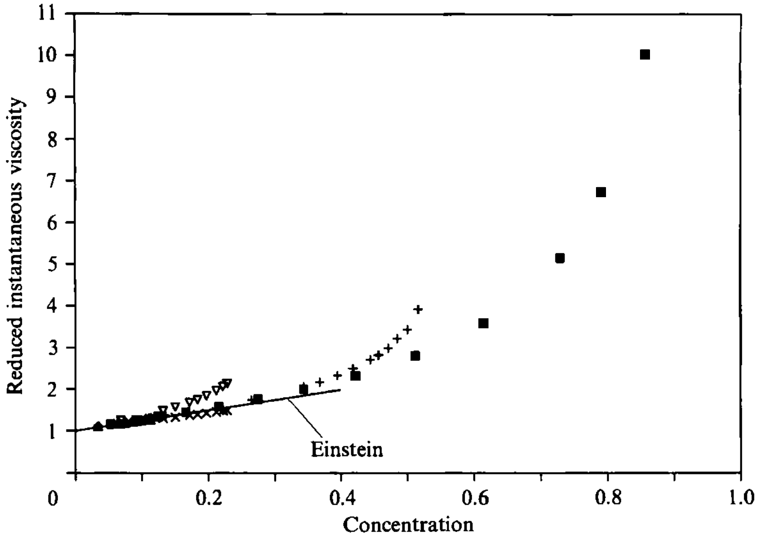

FIGURE 5. The instantaneous viscosity versus the volume fraction for cubic arrays of cubes (aligned perfectly with the unit cell) and spheroids. At volume fractions less than 0.4, a cubic array of cubes has about the same instantaneous viscosity as a cubic array of spheres. The same can be said of cubic arrays of spheroids at volume fractions not near to their maximum volume fractions. ■, cube; +, sphere; ◇, prolate spheroid aligned in the x- and z-directions; △, prolate spheroid aligned in the y-direction; ×, oblate spheroid aligned in the x- and z-directions; ▽, oblate spheroid aligned in the y-direction.

with the unit cell is plotted versus the volume fraction in figure 5. Instantaneous effective viscosities of spheroids are also plotted in the same figure for comparison.

At low volume fractions ($\Phi < 0.4$), the effective viscosity for an array of cubes is about the same as the effective viscosity for an array of spheres. In fact, the angular velocity (Ω_y) of the cube, over the whole volume fraction considered, should be exactly $0.5\dot{\gamma}$ as in the sphere case following from the symmetry arguments employed by Nunan & Keller (1984). The weak dependence of the averaged properties of suspensions on the shapes of the suspended particles, provided that the 'aspect ratio' of the particles is about one, has been noted before, for example, in the review by Metzner (1985). He showed that viscosity data on different suspensions of spheres, and rough crystals, can be correlated using a single empirical relation. At high volume fractions, we expect the particle shape to have a more dramatic effect in the effective viscosity. For a cubic array of perfectly aligned cubes, the lubrication force between the surfaces of two generic cubes has two components; one parallel to the surfaces and is proportional to a/h (the shearing force due to the relative motion between the two surfaces), and the other perpendicular to the surfaces and is proportional to $(a/h)^3$ (the squeezing force between two parallel surfaces), where h is the distance between the two surfaces. The relative motion of the surfaces of the cubes is neither parallel nor perpendicular to the cubes' surfaces, but it involves both translational and rotational motion. Since the effective viscosity is directly related to the lubrication force, and

$$\frac{h}{a} \propto \frac{1-(\Phi/\Phi_{max})^{\frac{1}{3}}}{(\Phi/\Phi_{max})^{\frac{1}{3}}},$$

we expect the effective viscosity to be proportional to ϵ^{-n}, where $\epsilon = 1-(\Phi/\Phi_{max})^{\frac{1}{3}}$, and $n = 1$ or 3 depending on whether the shearing or the squeezing action is

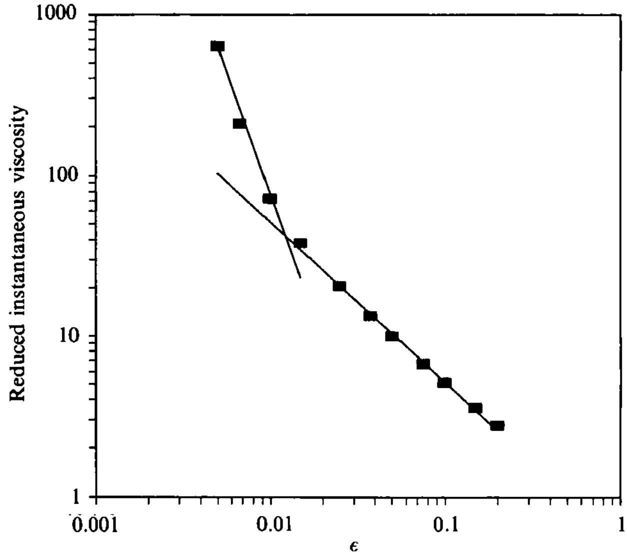

FIGURE 6. The instantaneous viscosity of a cubic array of perfectly aligned cubes at high volume fractions. The solid lines are the lines $7.9\times10^{-5}/\epsilon^3$, for $\epsilon < 0.01$ ($\Phi > 0.97$), and $0.52/\epsilon$, for $0.01 < \epsilon < 0.3$ ($0.34 < \Phi < 0.97$).

dominant, respectively. A numerical confirmation of this is given in figure 6: for $\epsilon < 0.01$ ($\Phi > 0.97$), the effective viscosity is given approximately by $7.9\times10^{-5}/\epsilon^3$. At moderate to high volume fractions, however, the effective viscosity is proportional to $1/\epsilon$, given by approximately $0.52/\epsilon$.

The singular nature of the effective viscosities of regular arrays is due to the fact that a snapshot in time is taken; the lubrication force between the two surfaces of the two generic particles allows this singularity to develop. If a dynamic simulation is attempted, however, and a time average of the instantaneous effective viscosity is taken, then, as shown by Adler *et al.* (1985), this time-averaged effective viscosity remains finite at all concentrations. The asymptotic results at high volume fractions for periodic arrays therefore must have limited applicability. These results, however, are useful as a validation of the numerical method.

We also perform some numerical experiments on cubic arrays of cubes by randomly assigning two Euler's angles to the suspended cubes and calculating the instantaneous effective viscosity of the suspension over the available range of volume fraction (which depends on the configuration of the cube). The results for nine different random configurations of the suspended cube are summarized in figure 7. It is interesting to note that the effective viscosity of a cubic array of perfectly aligned cubes is always lower than that of misaligned cubes. However, the instantaneous effective viscosity of a cubic array of spheres falls within the spread of the cube data. It would be more economical numerically to deal with a suspension of cubes, or other crystalline shapes (e.g. octahedra), since the number of elements needed is considerably smaller than that required to model a sphere, for the same accuracy. We note that the presence of sharp corners does not seem to cause any problem with the present numerical method at low to moderate volume fractions. At high volume fractions, where the corners or edges of one cube approach the face of another cube, the mobility function must approach zero, but this lubrication limit cannot be handled well with the present method. Our calculations stop well short of this limit.

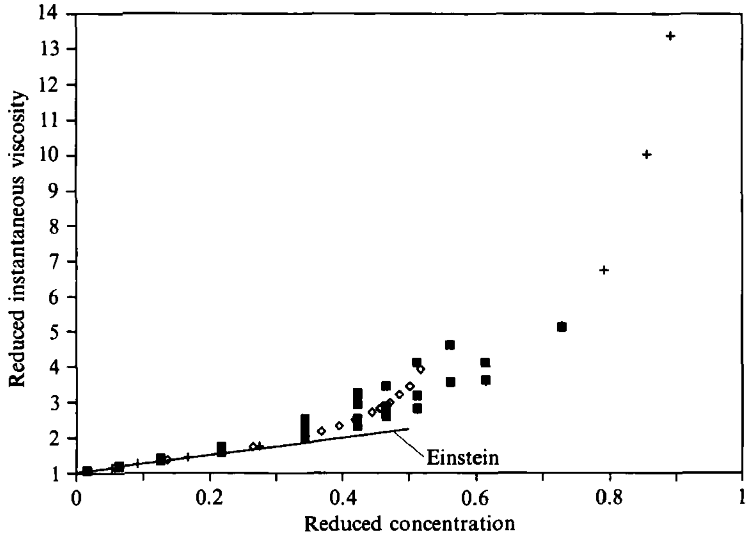

FIGURE 7. The instantaneous viscosity of a cubic array of cubes. The cube is randomly oriented with respect to the unit cell. Calculations with 9 different random orientations were carried out. ■, cube at different orientations; +, cube aligned with the unit cell; ◇, sphere.

3.5. *Cubic array of clusters of spheres*

The remainder of this paper is devoted to a few periodic arrays of clusters of two, three, four, and six spheres in a bulk shearing flow. Five cases are considered:

Case a: Cubic array of two spheres. The spheres' centres are placed at $(\pm a, 0, 0)$, where a is the sphere radius. The unit cell for this case can be further reduced to a parallelepiped containing one single sphere.

Case b: Cubic array of two spheres. The spheres' centres are placed at $(-a/\surd 2, 0, a/\surd 2)$ and $(a/\surd 2, 0, -a/\surd 2)$, respectively.

Case c: Cubic array of three spheres. The spheres centres are placed at $(-a, \pm a, 0)$ and $(a, 0, 0)$.

Case d: Cubic array of four spheres. The spheres' centres are placed at $(\pm \mathrm{a}, \pm \mathrm{a}, 0)$. This case is similar to case a in that it is possible to reduce to unit cell to a parallelepiped containing just one single sphere.

Case e: Cubic array of six spheres. The spheres' centres are placed at $(\pm a, \pm a, 0)$, and $(0, 0, \pm a\surd 3)$.

In all cases, the size of the unit cell is varied to cover the volume fraction of interest. The contours of velocities show that the flow mainly takes place in the xz-plane, with the y-component velocity of the order 10^{-2} or less, in all cases. Since cases a and d are not much different from a cubic array of spheres, they are expected to, and indeed do, behave like a cubic array of spheres, as far as effective properties are concerned. All spheres are modelled with 80 surface elements, and the surface of the unit cell is modelled with 300 elements.

The main results are summarized in figure 8, where the instantaneous effective viscosity is plotted against the volume fraction. It is apparent that case a and case d have about the same effective viscosities as the cubic array of spheres, all other cases have higher instantaneous effective viscosities. A plausible explanation of the observed higher viscosity is the immobilized liquid concept proposed by Vand (1948).

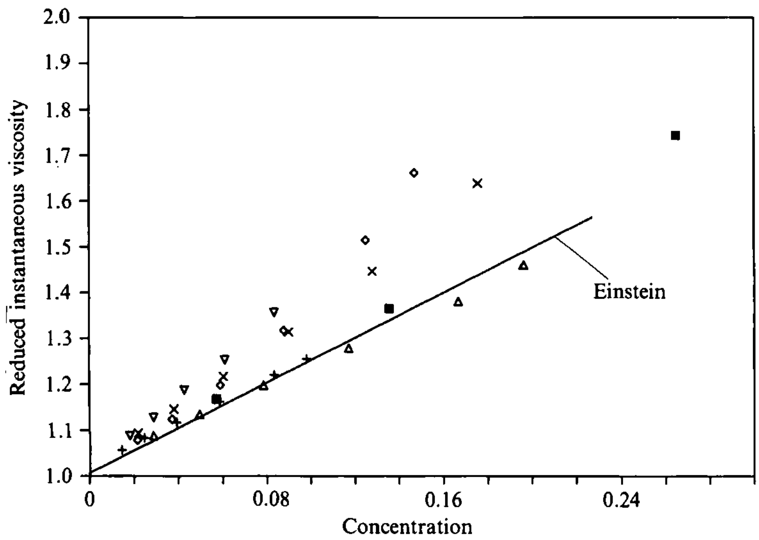

FIGURE 8. The instantaneous viscosity of cubic arrays of clusters of spheres. ■, cubic array of spheres; +, case *a* 2-sphere cluster; ▽, case *b* 2-sphere cluster; ◇, case *c* 3-sphere cluster; △, case *d* 4-sphere cluster; ×, case *e* 6-sphere cluster.

He proposed that in a cluster of particles, the liquid in the neighbourhood of the points of contact of the particles is effectively 'immobilized'. This immobilized liquid would then contribute to an effective volume fraction, Φ_{eff}, which is greater than the actual volume fractions of the particles. Roscoe (1952) extended Vand's concept of immobilized liquid and showed that if all the spheres are in clusters with four or more particles in a close-packed arrangement, then the effective volume fraction is $\Phi_{eff} = \Phi/\Phi_{max}$, where Φ_{max} is the maximum volume fraction for the type of packing of the clusters. This semi-empirical relation seems to work quite well (Graham, Steele & Bird 1984). Another set of data that support the concept of immobilized liquid was reported by Lewis & Nielsen (1968), who agglomerated small glass beads into irregular aggregates of as many as 250 particles. These aggregates were formed by sintering, hence they were permanent. They found that the data can be well correlated, provided that the volume fraction is that of the aggregated spheres plus the liquid imbibed in the interstices of the permanent aggregates.

We find that, by using an effective volume fraction $\Phi_{eff} \approx 1.5\Phi$, the instantaneous effective viscosities of the cases *b*, *c*, and *e* can be collapsed into a single curve. The front factor 1.5 would correspond to a body-centred cubic array for the cluster, according to Roscoe (1952). This is a reasonable type of packing for the six-sphere cluster (case *e*), but it is clearly inappropriate for case *b* and case *c*. In the latter cases, one can enclose the two-sphere and the three-sphere clusters in an envelope and calculate the effective volume fraction assuming that the fluid trapped in the envelop is immobilized. This leads to an effective volume fraction of 1.25Φ for the two-sphere cluster, and 1.34Φ for the three-sphere cluster. These values are considerably lower than the value found numerically. Thus the immobilized fluid concept works for some types of packing, but it may be too over-simplified to bring out minor effects, which, however, may have large effects on the macroscopic properties.

The rigid-body motion of the six spheres in the cluster is given in table 2 at $\Phi = 0.102$. The four spheres lying the plane $z = 0$ spin about the y-axis with an angular

Sphere's centre	U_x	U_y	U_z	Ω_x	Ω_y	Ω_z
$(a, a, 0)$	−0.001	−0.001	−0.39	0.06	0.43	−0.0003
$(-a, a, 0)$	0.001	−0.002	0.39	−0.06	0.43	0.0008
$(-a, -a, 0)$	−0.005	−0.001	0.39	0.06	0.43	−0.003
$(a, -a, 0)$	−0.006	0.00006	−0.39	−0.06	0.43	0.0001
$(0, 0, -a(1+3^{\frac{1}{2}}))$	−0.90	−0.002	−0.006	−0.001	0.68	−0.001
$(0, 0, a(1+3^{\frac{1}{2}}))$	0.90	−0.005	−0.007	0.0005	0.68	−0.002

TABLE 2. Rigid-body motion of the spheres in the 6-sphere cluster, $\Phi = 0.102$. The results are rounded up to at most two significant figures.

velocity of $0.43\dot{\gamma}$ and translate along the z-axis with velocities of $\pm 0.4a\dot{\gamma}$. The upper and lower spheres spin about the y-axis with an angular velocity of about $0.7\dot{\gamma}$ and translate along the x-axis with velocities of ± 0.9. At the instant considered, the cluster therefore spins with an averaged angular velocity of about 0.4. Whether or not the cluster can be maintained at a later time can only be determined by a dynamic simulation, which is not within the scope of the present study.

4. Concluding remarks

A successful application of the standard boundary-element method to solve Stokes flows past a periodic array of force- and torque-free particles is demonstrated. Simple cubic arrays of spheres, spheroids, cubes, and clusters of spheres are subjected to a bulk simple shearing flow. The effective volume-averaged stress tensor as well as the detailed kinematics and stress field throughout the Newtonian suspending fluid are obtained by post-processing the boundary solution. For a cubic array of spheres, the boundary element results agree well with the numerical and asymptotic results of Nunan & Keller (1984) up to 95% of the close packing volume fraction, even for a very coarse meshing. New results for cubic arrays of spheroids of aspect ratio of two and cubes show that the effective properties are weakly dependent on the particle shape. This weak dependency has some experimental support in some suspensions (Metzner 1985) and falling-ball rheometry (Mondy *et al.* 1987). At high volume fractions, the effective viscosity of a cubic array of perfectly aligned cubes behaves like $1/\epsilon^3$, where $\epsilon = 1-\Phi/\Phi_{\max} \rightarrow 0$. This singularity can be explained by lubrication forces between the two flat surfaces of the two cubes in the limit of high volume fractions.

Some results for clusters of a small number of spheres are also reported, which partially support the 'immobilized' liquid concept proposed by Vand (1948). The effective volume fraction is found to be about 1.5Φ, which is about the value proposed by Roscoe (1952), if the cluster is in a body-centred cubic packing.

The limitation of the current boundary-element method is the treatment (or the lack) of near particle interaction, which leads to ill-conditioned problems at a high level of discretization. It is precisely the near particle interaction that is essential in a dynamic simulation of suspensions, where particles inevitably come into very near contact. The boundary element method, however, can be used to generate results for a small number of particles (of the order of 100), which can be used to validate approximate methods designed to handle a very large number of particles in a realistic suspension.

This research is funded by an Australian Research Grant Scheme. The support is gratefully acknowledged. Portions of this work were supported by a grant from the Division of Engineering and Geosciences, Office of Basic Energy Science, US Department of Energy (KC04106). Work performed at Los Alamos Laboratory was sponsored by the US Department of Energy under contract W-7405-ENG-36 with the University of California. N.P.-T. wishes to thank the Staff of the Technical Engineering Support Group at Los Alamos for providing the facilities and support that allowed this study to be performed. We wish to thank Professor John F. Brady and the referees for their numerous suggestions to improve this paper.

REFERENCES

Adler, P. M., Zuzovsky, M. & Brenner, H. 1985 *Intl J. Multiphase Flow* **11**, 387.

Banerjee, P. K. & Butterfield, R. 1981 *Boundary Element Methods in Engineering Sciences*. McGraw-Hill.

Batchelor, G. K. 1970 *J. Fluid Mech.* **41**, 545.

Batchelor, G. K. 1976 *J. Fluid Mech.* **74**, 1.

Batchelor, G. K. 1982 *J. Fluid Mech.* **119**, 379.

Beenakker, C. W. J. 1984 *Physica* **128**, 48.

Bloomfield, V., Dalton, W. O. & Holde, K. E. van 1967 *Biopolymers* **5**, 135.

Brady, J. F. & Bossis, G. 1988 *Ann. Rev. Fluid Mech.* **20**, 111.

Brady, J. F., Phillips, R. J., Lester, J. C. & Bossis, G. 1988 *J. Fluid Mech.* **195**, 257.

Brebbia, C. A., Telles, J. F. C. & Wrobel, L. C. 1984 *Boundary Element Techniques*. Springer.

Brenner, H. 1963 *Chem. Engng Sci.* **18**, 1.

Brenner, H. 1964*a* *Chem. Engng Sci.* **19**, 599.

Brenner, H. 1964*b* *Chem. Engng Sci.* **19**, 631.

Brenner, H. 1964*c* *Chem. Engng Sci.* **19**, 703.

Brenner, H., Nadim, N. & Haber, S. 1987 *J. Fluid Mech.* **183**, 511.

Brenner, H. & O'Neill, M. E. 1972 *Chem. Engng Sci.* **27**, 1421.

Bush, M. B. & Phan-Thien, N. 1984 *J. Non-Newt. Fluid Mech.* **16**, 303.

Durlofsky, L., Brady, J. F. & Bossis, G. 1987 *J. Fluid Mech.* **180**, 21.

Ganatos, P., Pfeffer, R. & Weinbaum, S. 1978 *J. Fluid Mech.* **84**, 79.

Gluckman, M. J., Pfeffer, R. & Weinbaum, S. 1971 *J. Fluid Mech.* **50**, 705.

Gluckman, M. J., Weinbaum, S. & Pfeffer, R. 1972 *J. Fluid Mech.* **55**, 677.

Graham, A. L., Steele, R. D. & Bird, R. B. 1984 *Indust. Engng Chem. Fund.* **23**, 421.

Happel, J. & Brenner, H. 1973 *Low Reynolds Number Hydrodynamics*. Noordhoff.

Hasimoto, H. 1959 *J. Fluid Mech.* **5**, 317.

Herczyński, R. & Pieńkowska, I. 1980 *Ann. Rev. Fluid Mech.* **12**, 237.

Ingber, M. S., Mondy, L. A. & Graham, A. L. 1989 *61st Ann. Meeting Soc. Rheol. Montreal, Canada.*

Jeffery, G. G. 1922 *Proc. R. Soc. Lond.* A**102**, 161.

Jeffrey, D. J. & Acrivos, A 1976 *AIChE J.* **22**, 417.

Jeffrey, D. J. & Onishi, Y. 1984 *J. Fluid Mech.* **139**, 261.

Karrila, S J. & Kim, S. 1990 *Rheology Research Center Report RRC* 123, University of Wisconsin, Madison.

Kim, S. 1987 *Phys. Fluids* **30**, 2309.

Kim, S., Fuentes, Y. O. & Karrila, S. J. 1990 *Stat. Phys.* in press.

Kim, S. & Mifflin, R. T. 1985 *Phys. Fluids* **28**, 2033.

Kirkwood, J. G. & Riseman, J. 1948 *J. Chem. Phys.* **16**, 565.

Kynch, G. J. 1959 *J. Fluid Mech.* **5**, 193.

Leichtberg, S., Pfeffer, P. & Weinbaum, S. 1976*a* *Intl J. Multiphase Flow* **3**, 147.

LEICHTBERG, S., WEINBAUM, S., PFEFFER, P. & GLUCKMAN, M. J. 1976*b* *Phil. Trans. R. Soc.* A **282**, 585.

LEWIS, T. B. & NIELSEN, L. E. 1968 *Trans. Soc. Rheol.* **12**, 421.

MCCAMMON, J. A. & DEUTCH, J. M. 1976 *Biopolymers* **15**, 1397.

MAZUR, P. & SAARLOOS, W. VAN 1982 *Physica* **115**, 21.

METZNER, A. B. 1985 *J. Rheol.* **29**, 739.

MONDY, L. A., GRAHAM, A. L., STROEVE, P. & MAJUMDAR, A. 1987 *AIChE J.* **33**, 862.

NUNAN, K. C. & KELLER, J. B. 1984 *J. Fluid Mech.* **142**, 269.

PHAN-THIEN, N., TRAN-CONG, T. & RAMIA, M. 1987 *J. Fluid Mech.* **184**, 533.

ROGER, R. P. & HUSSEY, R. G. 1982 *Phys. Fluids* **25**, 915.

ROSCOE, R. 1952 *Brit. J. Appl. Phys.* **3**, 267.

SAFFMAN, P. G. 1973 *Stud. Appl. Maths* **52**, 115.

SWANSON, E., TELLER, D. C. & HAËN, C. DE 1978 *J. Chem. Phys.* **68**, 5097.

TRAN-CONG, T. & PHAN-THIEN, N. 1988*a* *Rheol. Acta* **27**, 21.

TRAN-CONG, T. & PHAN-THIEN, N. 1988*b* *Rheol. Acta* **27**, 301.

TRAN-CONG, T. & PHAN-THIEN, N. 1988*c* *J. Non-Newt. Fluid Mech.* **30**, 37.

TRAN-CONG, T. & PHAN-THIEN, N. 1989 *Phys. Fluids* A**1**, 453.

TRAN-CONG, T., PHAN-THIEN, N. & GRAHAM, A. L. 1990 *Phys. Fluids* A**2**, 666.

VAND, V. 1948 *J. Phys. Colloid Chem.* **52**, 277.

YOUNGREN, G. K. & ACRIVOS, A. 1975 *J. Fluid Mech.* **69**, 377.

ZICK, A. A. & HOMSY, G. M. 1982 *J. Fluid Mech.* **115**, 13.

ZUZOVSKY, M. 1976 Transport processes in spatially periodic suspensions. PhD thesis, Carnegie–Mellon University [76-30188].

ZUZOVSKY, M., ADLER, P. M. & BRENNER, H. 1983 *Phys. Fluids* **26**, 1714.